Author's personal copy

Remote Sensing of Environment 115 (2011) 2141–2151

Contents lists available at ScienceDirect

Remote Sensing of Environment

journal homepage: www.elsevier.com/locate/rse

LAI assessment of wheat and potato crops by VENμS and Sentinel-2 bands

I. Herrmann [a], A. Pimstein [a,1], A. Karnieli [a,*], Y. Cohen [b], V. Alchanatis [b], D.J. Bonfil [c]

[a] The Remote Sensing Laboratory, Jacob Blaustein Institutes for Desert Research, Ben-Gurion University of the Negev, 84990, Israel
[b] Institute of Agricultural Engineering, Agricultural Research Organization, Volcani Center, Bet Dagan, Israel
[c] Field Crops and Natural Resources Department, Agricultural Research Organization, Gilat Research Center, Israel

ARTICLE INFO

Article history:
Received 14 July 2010
Received in revised form 6 April 2011
Accepted 10 April 2011
Available online 8 May 2011

Keywords:
LAI
Red-edge
Agriculture
NDVI
PLS
VIP
VENμS
Sentinel-2

ABSTRACT

Leaf Area Index (LAI) is an important variable that governs canopy processes and can be monitored by satellites. The current study aims at exploring the potential and limitations of using the red-edge spectral bands of the forthcoming superspectral satellites, namely—Vegetation and Environmental New micro Spacecraft (VENμS) and Sentinel-2, for assessing LAI in field crops. The research was conducted in experimental plots of wheat and potato in the northwestern Negev, Israel. Continuous spectral data were collected by a field spectrometer and LAI data were obtained by a ceptometer. The spectral data were resampled to the superspectral VENμS and Sentinel-2 resolutions. The data were divided into seven datasets (four seasons, two crops, and one including all data). The LAI prediction abilities by Partial Least Squares (PLS) models for continuous spectra and the resampled spectra were compared and evaluated. For wheat and potato of the continuous, VENμS, and Sentinel-2 data formations, the PLS correlation coefficients (r) values were 0.93, 0.93, and 0.92, respectively. In most cases, the red-edge region was found to be the most important spectral region for the three data formations, according to the Variable Importance in Projection (VIP) analysis. Additionally, Normalized Difference Vegetation Index (NDVI) and the Red-Edge Inflection Point (REIP) were computed for the three data formations in order to observe relation to as well as prediction accuracy in retrieving LAI values. The prediction abilities of the calculated indices by the data formations were compared, peaking for wheat, with r values of 0.91 for the REIP for the three data formations. Therefore, it is concluded that VENμS and Sentinel-2 can spectrally assess LAI as good as a hyperspectral sensor. The REIP was found to be a significantly better predictor than NDVI for wheat data and therefore can potentially be implemented for future LAI monitoring applications by superspectral sensors that contain four red-edge bands.

© 2011 Elsevier Inc. All rights reserved.

1. Introduction

Leaf Area Index (LAI) was defined by Watson (1947) as *the total one-sided area of leaf tissue per unit ground surface area*, giving a dimensionless value, typically ranging from 0, for bare ground, to more than 7 for dense vegetation (Darvishzadeh et al., 2008). LAI is one of the most important variables governing canopy processes and is related to leaf and canopy chlorophyll contents, photosynthesis rate, carbon and nutrient cycles, dry and fresh biomass, and growth stages (Aparicio et al., 2002; Baret et al., 1992; Clevers et al., 2001; Coyne et al., 2009; Darvishzadeh et al., 2008; Pimstein et al., 2009; Pu et al., 2003; Ye et al., 2008). Hence, LAI is applied in plant and environmental studies of evaporation, transpiration, light absorption, yield estimation, growth stages of crops, and chemical element cycling (Aparicio et al., 2002; Delegido et al., 2008; Kimura et al., 2004; McCoy, 2005; Moran et al., 2004). LAI has been extensively monitored in agricultural crops and forest studies either through statistical approaches or by deriving canopy reflectance models from remotely sensed data. However further research on the accuracy of the existing algorithms in present and future platforms is required (Aparicio et al., 2002; Asrar et al., 1984; Darvishzadeh et al., 2008; Gitelson, 2004; Kimura et al., 2004; Pimstein et al., 2009; Pu et al., 2003). A common non-destructive surrogate for LAI, which is based on reflectance of red (R) and near infrared (NIR) bands, is the Normalized Difference Vegetation Index (NDVI). However, when correlated with LAI, NDVI tends to exhibit less sensitivity for LAI values that are higher than 2 (Aparicio et al., 2002; Asrar et al., 1984; Coyne et al., 2009; Gitelson, 2004; le Maire et al., 2008; Zarco-Tejada et al., 2005). This NDVI-LAI insensitivity will be referred to hereafter as 'saturation'. To overcome this drawback, there is a need to use other spectral relations. One example is the Wide Dynamic Range Vegetation Index (WDRVI; Gitelson, 2004). Gitelson (2004) introduced the WDRVI, which is

* Corresponding author at: The Remote Sensing Laboratory, Jacob Blaustein Institutes for Desert Research, Ben Gurion University of the Negev, Sede Boker Campus 84990, Israel. Tel.: +972 8 6596855; fax: +972 8 6596805.
E-mail address: karnieli@bgu.ac.il (A. Karnieli).
[1] Current address: Departamento de Fruticultura y Enología, Facultad de Agronomía e Ingeniería Forestal, Pontificia Universidad Católica de Chile, Av. Vicuña Mackenna, 4860 Santiago, Chile.

0034-4257/$ – see front matter © 2011 Elsevier Inc. All rights reserved.
doi:10.1016/j.rse.2011.04.018

Author's personal copy

linearly related to LAI, by applying the same bands as NDVI and adding a weighting coefficient, obtained by trial and error, for the NIR bands. Although the WDRVI was originally designed for the Advanced Very High Resolution Radiometer (AVHRR), Gitelson (2004) recommended to adapt it to other satellites. Another example is the Red-Edge Inflection Point (REIP) after Guyot & Baret (1988).

The red-edge can be mathematically defined as the inflection point position, in terms of wavelengths, on the slope connecting the local minimum reflectance in the R and the maximum reflectance in the NIR spectral regions (Dawson & Curran, 1998; Mutanga & Skidmore, 2007; Pu et al., 2003). Physiologically, this steep increase of reflectance marks the transition between the photosynthetically affected region of the spectrum (maximum absorption of chlorophyll *a* and *b* at 662 nm and 642 nm, respectively), and the region with high reflectance values of the NIR plateau affected by plant cell structure or leaf layers. This feature enables a clear representation of chlorophyll absorption dynamics, illustrating a shoulder shift towards longer wavelengths when the chlorophyll absorption increases (higher chlorophyll content) and a shift towards the shorter wavelengths with decreasing chlorophyll absorption (Moran et al., 2004). Thus, the position of the red-edge, in canopy scale, provides an indication of plant condition that might be related to a variety of factors as LAI, nutrients, water and chlorophyll contents, seasonal patterns, and canopy biomass (Baret et al., 1992; Blackburn & Steele, 1999; Buschmann & Nagel, 1993; Cho & Skidmore, 2006; Clevers et al., 2001; Dawson & Curran, 1998; Delegido et al., 2008; Jorgensen, 2002; Moran et al., 2004; Pu et al., 2003; Tarpley et al., 2000). Baret et al. (1992) simulated canopy scale reflectance using the SAIL radiative transfer model based on Verhoef (1984), concluding that information provided by shifts in the red-edge is not equivalent to broad band R and NIR reflectance values. Buschmann & Nagel (1993) indicated that high spectral resolution is required for determining the inflection point and this is therefore unpractical for low-spectral resolution sensors. This leads to the understanding that unique spectral resolutions should be considered in order to obtain red-edge data by non-hyperspectral sensors. Clark et al. (1995) confirmed the latter by observing a red-edge shift in several fields with different crops, growing stages and variety of stresses, obtained by the hyperspectral airborne sensor Airborne Visual and Infra-Red Imaging Spectrometer (AVIRIS). Multispectral or superspectral (more than ten and less than 50 bands, i.e., in-between multispectral and hyperspectral resolutions) sensors that aim at high quality precision agricultural red-edge applications, should introduce a unique combination of spectral and spatial resolutions as well as revisit time.

Due to importance of the above-mentioned variables for vegetation monitoring in general, and for agriculture in particular, many spectral indices have been derived to assess and correlate these variables with the state and condition of different crops. In recent years, most of the high spatial resolution operational satellites (e.g., Ikonos, QuickBird, RapidEye, GeoEye, WorldView-2) have aimed at providing reasonable solutions for precision agriculture, however these satellites are characterized by a small number of broad spectral bands, usually in the blue (B), green (G), R, and NIR regions. In the WorldView-2 system a single red-edge band is available but it is not suitable for retrieving the REIP. It is worth mentioning that only one operational superspectral spaceborne system, MERIS, has four red-edge bands out of 15 bands ranging from 390 to 1040 nm with programmable bandwidth ranging from 2.5 to 30 nm. These four bands are centered at 681.25, 708.75, 753.75, and 760.625 nm and commonly set to bandwidths of 7.5, 10, 7.5, and 3.75 nm, respectively. However, this system is characterized by a spatial resolution of 300 m and therefore is not suitable for small scale (precision) agricultural applications.

The forthcoming superspectral satellite Sentinel-2 to be launched in 2012 is intended for environmental, including agricultural, applications. Among its 13 bands, it includes four red-edge bands centered at 665, 705, 740, and 783 nm with bandwidth of 30, 15, 15, and 20 nm, as presented in Table 1, and a spatial resolution of 10, 20, 20, and 20 m, respectively. This satellite will circulate in a near polar sun-synchronous orbit at 786 km above Earth with 290 km swath. The Sentinel-2 mission will include twin satellites 180° apart from one another providing a global revisit time of five days (two days in extended mode).

Another future superspectral spaceborne system, named Vegetation and Environmental New micro Spacecraft (VENμS) will be launched in 2013. This system is characterized by a tilting sensor (30° along and across track) with high spatial (5.3 m), spectral (12 spectral bands in the visible (VIS)–NIR), and temporal (two day revisit time with the same viewing angle) resolutions. Among its 12 bands, it includes four bands along the red-edge, centered at 667, 702, 742, and 782 nm, with bandwidths of 30, 24, 16, and 16 nm, respectively, as presented in Table 2. VENμS will circulate in a near polar sun-synchronous orbit at 720 km above Earth and will acquire images over planned sites of 27 km swath. Because of these combined unique capabilities, the primary objective of this system is vegetation monitoring. Moreover, it will be specifically suitable for precision agriculture tasks such as site-specific management that can be applied with decision support systems.

Fig. 1 presents the location of the spectral bands of both satellites, VENμS and Sentinel-2 that are relevant to this study. Also presented is the transmittance of electromagnetic radiation in the range of 400 to 1000 nm, obtained from mid-latitude Modtran product of total atmospheric gases (e.g., water vapor, oxygen, carbon dioxide). VENμS band number 12 and Sentinel-2 band number 9 are located in one of the atmospheric water vapor absorption features in order to allow water vapor detection. The rest of the bands of both satellites were carefully located in-between the main gas absorptions in order to provide data with minimal atmospheric effect. In Fig. 1, the canopy reflectance spectra are typical potato and wheat spectra that will be discussed later. This data combination in Fig. 1 allows observing the relevance of the satellite bands to potential applications for canopy reflectance values of the entire spectra as well as vegetation indices.

This study aims at demonstrating the potential of future superspectral satellites to retrieve LAI values in wheat and potato crops using the VIS—red-edge—NIR spectral regions by entire spectra as well as by the REIP in comparison with the NDVI.

2. Methodology

2.1. Study area

Wheat and potato experiments were established in the northwestern Negev, Israel, between 2003 and 2007. The wheat experiment took place in experimental plots applying different nitrogen fertilization levels, irrigation treatments, and seeding densities (Pimstein et al., 2007b) at Gilat Research Center (31° 21′ N; 34° 42′ E) and was conducted during two winter growing seasons, 2003–04 (2004) and 2004–05 (2005). The potato experiment took place in experimental plots applying different nitrogen fertilization levels (Cohen et al., 2010; Herrmann et al., 2010) in commercial fields at Kibbutz Ruhama (31°28′ N, 34°41′ E) and was conducted during two growing seasons in the autumn of 2006 and spring of 2007. A variety of treatments (i.e., nitrogen, water), for different leaf structures (i.e., grass and broadleaf), and along different growing stages, provided an assortment of LAI values. The LAI assessment for different treatments as well as growing stages is beyond the scope of the current paper.

2.2. Field measurements

Ground spectral reflectance measurements of canopy were acquired along with LAI measurements within the same field of view (FOV) of the spectral measurements. The measurements in the

Author's personal copy

Table 1
Sentinel-2 bands.

Band #	1	2	3	4	5	6	7	8	8a	9	10	11	12
Band center (nm)	443	490	560	665	705	740	783	842	865	945	1375	1610	2190
Bandwidth (nm)	20	65	35	30	15	15	20	115	20	20	30	90	180

wheat fields were obtained from 21 days after emergence (DAE), until the heading stage, i.e., 97 DAE (Pimstein et al., 2007a). The measurements in the potato field were obtained between 19 and 90 days after seeding (DAS). The detailed number of measurements during each sampling day and each growing season, for each crop is presented in Table 3. For analysis purposes, the data were divided into 7 different datasets: each growing season (i.e., 4 datasets); each crop (i.e., 2 datasets); and all the data together (i.e., 1 dataset).

Each spectral measurement was followed by three LAI measurements that were averaged to one LAI value. Therefore, each spectrum is coupled with one LAI value. Canopy reflectance measurements were obtained using Analytical Spectral Devices (ASD) FieldSpec Pro FR spectrometer with a spectral range of 350–2500 nm and 25° FOV. The spectral sampling resolution is 1.4 nm for 350–1000 nm and 2 for 1000–2500 nm. The spectral measurements were collected ± 2 h from solar noon, under clear sky, and in nadir orientation. The spectrometer was programmed to automatically calculate the average of 20 readings that were taken at each sampling point. The measurements were collected 1.5 m above the ground, generating an instantaneous FOV (IFOV) of about 0.35 m^2. During the season, as the height of the crops increased, the sensor's distance from the top of the canopy diminished from almost 1.5 to 0.7 m for wheat canopy and from 1.3 to 0.9 m for potato canopy. The height differences correspond to an IFOV 0.08 m^2 and 0.13–0.26 m^2, for the two crops respectively. Standard white reference panel (Spectralon Labsphere Inc.) was used as a white reference for the wheat spectral data acquisition while for the potato spectral data collection, pressed and smoothed barium sulfate ($BaSO_4$) powder was used for the same purpose (Hatchell, 1999). The LAI was measured by the AccuPAR LP-80 ceptometer (Decagon Devices, Inc), with an 86.5 cm long probe. The ceptometer was programmed differently, according to each crop and location based on the manufacturer's instructions. The leaf distribution parameter (x), needed for the LAI computation by the ceptometer, referring to the distribution of leaf angles within canopy, was set differently for each crop; 0.96 for wheat and 2.00 for potato (Decagon Devices, 2003).

2.3. Data analysis

2.3.1. Spectral data

Preprocessing the spectral data included eliminating atmospheric water absorption regions, namely 1.35–1.42 and 1.80–1.96 μm, as mentioned by Pimstein et al. (2009) as well as linear interpolation of the data to 1 nm and 2 nm narrow bands. The 2 nm spectral data are denoted hereafter as continuous spectra. The 1 nm spectral data were resampled to VENμS and Sentinel-2 spectral bands and denoted hereafter as VENμS and Sentinel-2 spectra. The resampling of the 1 nm narrow bands reflectance spectra to the satellites bands was executed by averaging the reflectance values of all wavelengths in the range of each band (Tables 1 and 2). For the Sentinel-2, bands 8 and 10–12 were ignored since they are not relevant for this work. Each of the seven datasets for each of the three data formations (continuous, VENμS, and Sentinel-2) was randomly divided into subsets—60% calibration and 40% validation. Partial Least Squares (PLS) analysis is a practical predictive tool for spectral reflective data (Hansen & Schjoerring, 2003; Nguyen & Lee, 2006). Since PLS prediction models can deal efficiently with the multi-collinearity present among the predictors (in this case wavelengths of spectral data), and analyze spectra when the number of wavelengths is either larger or smaller than the number of observations as well as deal with noisy spectra (Atzberger et al., 2010; Wold et al., 2001), the PLS models were applied for LAI prediction by the entire spectra for each of the datasets and data formations. The PLS analysis was applied with full cross-validation (Efron & Gong, 1983) by The Unscrambler® v.9.1 software. The prediction was evaluated by the Root Mean Square Error of Prediction (RMSEP) as well as by correlation coefficient (r) values of the relation between the predicted and observed LAI values. To determine whether there is a significant difference between coupled r values, two tailed *t*-test was applied by the Statistica v.9 software. In order to evaluate the relative importance of each waveband in each of the PLS models, the Variable Importance in Projection (VIP) after Wold et al. (1993) was computed. The VIP is defined as the summary of the importance for each predictor projections to find a number of principal components of the PLS model (Chong & Jun, 2005; Cohen et al., 2010). The VIP is computed as each predictor's importance with the explained sum of squares by the PLS dimension, summed for all dimensions related to the total explained sum of squares by the PLS model and for the total number of predictors. Therefore, it is an indicator of each predictor's (in this case wavelengths of spectral data) relative power in a PLS model. Hence the advantage of VIP over the regression coefficients of the PLS model in locating important predictors. The VIP can be used in case of multi-collinearity among the predictors. The VIP analysis was applied in a Matlab environment by the PLS toolbox of Eigenvector. The VIP values are evaluated by "the higher the better" where the average VIP = 1 is considered to be the putative threshold since it is the average value of the PLS model predictors' VIP values.

Table 2
VENμS bands.

Band #	1	2	3	4	5	6	7	8	9	10	11	12
Band center (nm)	420	443	490	555	620	620	667	702	742	782	865	910
Bandwidth (nm)	40	40	40	40	40	40	30	24	16	16	40	20

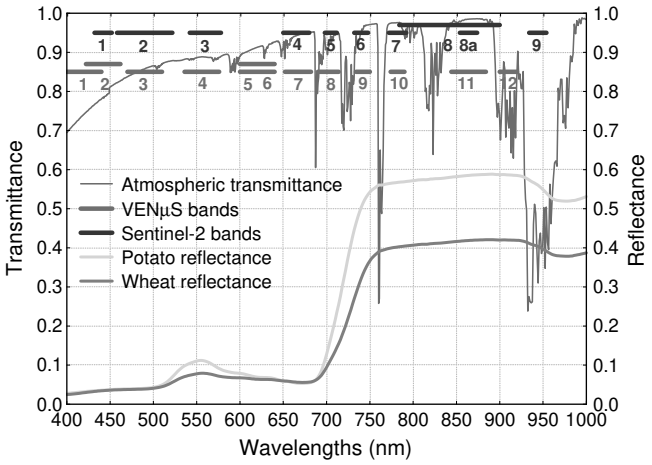

Fig. 1. Band settings of VENμS and Sentinel-2 with respect to the atmospheric transmittance and typical vegetation reflectance spectra.

Author's personal copy

Table 3
Measurement distribution by: crops, growing seasons, day after emergence (DAE) for wheat, and days after seeding (DAS) for potato. The first two digits represent either DAE or DAS and the digits in brackets the number of samples.

Datasets		Crops and growing season				Total number of samples
#	Name	Wheat		Potato		
		2004 winter	2005 winter	2006 autumn	2007 spring	
1	2007 potato	–	–	–	19(20); 41(19); 54(20); 77(20); 84(19); 91(19)	117
2	2006 potato	–	–	38(30); 50(30); 58(30); 78(30)	–	120
3	All potato	–	–	38(30); 50(30); 58(30); 78(30)	19(20); 41(19); 54(20); 77(20); 84(19); 91(19)	237
4	2005 wheat	–	47(24); 54(24): 63(24); 91(24)	–	–	96
5	2004 wheat	21(30); 45(24); 59(24): 72(24); 84(24); 97(24)	–	–	–	150
6	All wheat	21(30); 45(24); 59(24): 72(24); 84(24); 97(24)	47(24); 54(24): 63(24); 91(24)	–	–	246
7	All data	21(30); 45(24); 59(24): 72(24); 84(24); 97(24)	47(24); 54(24): 63(24); 91(24)	38(30); 50(30); 58(30); 78(30)	19(20); 41(19); 54(20); 77(20); 84(19); 91(19)	483

2.3.2. Vegetation indices

For the three data formations, two known vegetation indices were computed: NDVI (Rouse et al., 1974) and REIP linear four point interpolation approach, after Guyot & Baret (1988) and Clevers et al. (2001). Several methods for REIP calculation, such as Lagrangian interpolation technique (Dawson & Curran, 1998), inverted Gaussian model (Bonham-Carter, 1988), polynomial fitting (Pu et al., 2003), and first derivative (Mutanga & Skidmore, 2007), are mostly relied on hyperspectral data (Pu et al., 2003). The linear four point interpolation approach (Clevers et al., 2001; Guyot & Baret, 1988; Mohd-Shafri et al., 2006; Pu et al., 2003) was chosen since it is applicable for superspectral data and uses wavelengths available from VENμS and Sentinel-2 band formations. In Eqs. (1) to (4) ρ stands for reflectance in a certain wavelength of the continuous spectra, expressed in nanometers. Eq. (1) presents the wavelengths and band centers applied for computing NDVI. Eq. (2) presents the wavelengths for computing REIP by continuous spectra. Eqs. (3) and (4) present band center wavelengths of VENμS and Sentinel-2, respectively, applied for computing REIP. For computing the indices for the superspectral data formations, the wavelengths were substituted by the respective bands. VENμS band numbers applied for computing the NDVI and REIP were 7 and 10 and 7, 8, 9 and 10, respectively. Sentinel-2 band numbers applied for computing the NDVI and REIP were 4 and 7 and 4, 5, 6 and 7, respectively.

$$NDVI = \frac{\rho_{782} - \rho_{666}}{\rho_{782} + \rho_{666}} \quad (1)$$

$$REIP = 700 + 40\left\{\frac{[(\rho_{670} + \rho_{780})/2] - \rho_{700}}{\rho_{740} - \rho_{700}}\right\} \quad (2)$$

$$REIP = 702 + 40\left\{\frac{[(\rho_{667} + \rho_{782})/2] - \rho_{702}}{\rho_{742} - \rho_{702}}\right\} \quad (3)$$

$$REIP = 705 + 35\left\{\frac{[(\rho_{665} + \rho_{783})/2] - \rho_{705}}{\rho_{740} - \rho_{705}}\right\} \quad (4)$$

The index values were scatter-plotted against LAI to provide general sensitivity examination as well as to obtain the r values for linear relation between each index and LAI. The same calibration and validation subsets (as for the PLS analysis) were applied for LAI prediction by linear modeling for the seven datasets for both indices calculated by the three data formations. The RMSEP was calculated and the r values of the relation between the predicted and observed LAI values were presented in order to evaluate the quality of prediction. As before, *t*-test was applied in order to find out if there is a significant difference between coupled r values.

3. Results and discussion

3.1. Spectral data

Fig. 2 presents the continuous spectra for wheat and potato. Both crops have high reflectance variability in the NIR region (from 0.25 to

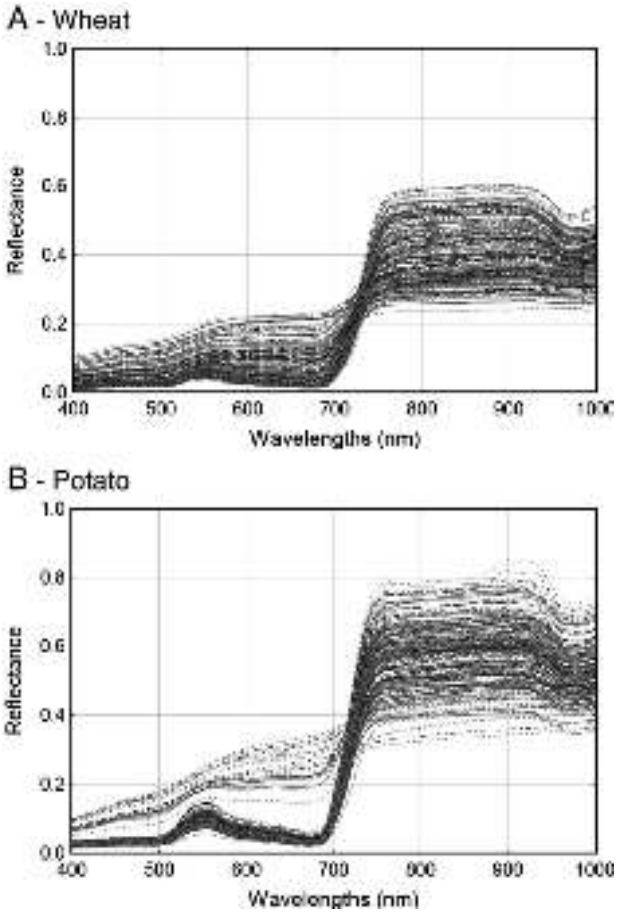

Fig. 2. Spectral variation of reflectance curves: (A) Wheat and (B) Potato.

Author's personal copy

0.6 and from 0.3 to 0.8 for wheat and potato, respectively). In the VIS region the range of the reflectance data for both crops is similar but the potato spectra seem to be grouped into two separate sections due to the nature of the different size, shape, density, and growth rate of the potato plants, although both crops have a similar number of samples during early growing stages (Table 3). It is also evident that the red-edge slope of the wheat spectra is much more variable than that of the potato. When observing the averaged continuous spectra of each crop, 246 samples for wheat and 237 for potato, the red-edge and NIR differences might be noticed (Fig. 1). The NIR plateau for the grass (wheat) spectra is about 30% lower than that of the broadleaf (potato) due to the internal structure, layers, and orientation of the leaves (Gausman, 1985; Raven et al., 2005).

3.2. PLS modeling

Table 4 presents the r and RMSEP values of LAI predicted by the entire spectra of the three data formations versus the observed LAI. All the r values are statistically significant ($p<0.001$). Nguyen and Lee (2006) obtained a similar r value for LAI prediction by PLS model for rice. Hansen and Schjoerring (2003) reported $r=0.87$ and RMSEP = 0.40 for LAI prediction by PLS model of wheat; these results are similar (more for the r values than the RMSEP) to the results for the three wheat datasets presented in Table 4. According to the RMSEP values there is no marked advantage for any of the data formations but in most cases there is an advantage for the super-spectral data formations over the continuous formation. Each of the probability (p) values is based on a *t*-test that computes the probability of the coupled r values to be the same, in order to compare the data formations. All *t*-test p values are higher than 0.05 (except for one case). Since there is no marked advantage for any of the data formations by the RMSEP values and according to the *t*-test p values the compared r values are the same, we find that there is no advantage for the continuous spectra over the VENμS or Sentinel-2 spectra. The coupled 'all wheat' and 'all potato' r values, for each of the data formations in Table 4 were t-tested for similarity and p values were 0.0008 for the continuous, 0.055 for VENμS, and 0.006 for the Sentinel-2 data formations. Hence the PLS model for 'all wheat' dataset can predict LAI better than the 'all potato' model. On the other hand, it should be mentioned that the RMSEP values for the 'all potato' dataset are smaller than the 'all wheat' dataset (Table 4). However since the range of LAI values for 'all potato' is 4.95 and for 'all wheat' is 6.99, the RMSEP should be compared as percentage out of these ranges. The RMSEP values for the potato and wheat of the continuous data formation are 11.5% and 8.5%, for the VENμS data formation the values are 11% and 9.7%, and for Sentinel-2 the values are 10.3% and 8.9%, respectively. Therefore, the model for 'all wheat' dataset can predict LAI better than the 'all potato' model. The differences between 'all wheat' and 'all potato' datasets will be further explored and discussed in Section 3.4.

Fig. 3 presents VIP values for the wavelengths and bands referring to the PLS models of entire spectra in relation to LAI applied for 'all data', 'all wheat', and 'all potato' datasets. In each of these figures the Y axis values are the VIP values of continuous, VENμS, and Sentinel-2 spectra, related to LAI. It can be seen that the red-edge region has notably the highest VIP values for the continuous spectra. Seeing that in most of the cases in Fig. 3 the VIP values of the superspectral sensors are very similar if not identical to the continuous VIP values, especially in the red-edge region, it can be assumed that if bands between 700 and 740 nm were available by both satellites, their VIP values would be similar to the continuous VIP values. For the VENμS spectra, the importance of the red-edge is competitive to the G region as presented in Fig. 3C for 'all potato' dataset and probably consequently also in the 'all data' dataset (Fig. 3A). The G advantage is probably due to the additional VENμS band centered at 620 nm providing data from the slope between G and R regions. It is worth mentioning that in Fig. 3B there is a shallow G peak of the continuous data that is detected only by the VENμS data. Therefore, high G region importance in the PLS model mentioned above might be related to the potato crop nature as expressed in the VIS region reflectance differences between wheat and potato (Fig. 2) presenting a steeper slope between the G and R regions in the case of the potato. For the Sentinel-2 wheat spectra (Fig. 3B) the NIR band centered at 865 nm is slightly more related to LAI variability than the red-edge. One of this band's declared purposes is LAI detection. The VENμS band centered at the same wavelength has the same VIP value as the Sentinel-2 band but lower VIP value than the red-edge. When examining Fig. 3B and C it can be seen that the three data formation VIP values are higher in the VIS region for potato while the NIR region has higher VIP values for the wheat. Therefore, the different canopy structure and biochemical constitution of the two species makes the VIS region, which is mostly affected by pigment constitution, more important in LAI determination of potato, while the NIR region, which is mostly affected by canopy structure, is more important for wheat LAI determination.

For the continuous spectra in Fig. 3, the peaks of the VIP values are centered at 720, 728, and 718 nm and the averaged REIP values of the 'all data', 'all wheat', and 'all potato' are 721, 723, and 719 nm, respectively (the same trend in averaged REIP of these three datasets is kept for both superspectral data formations). This difference between wheat and potato VIP peaks can be related to the shift in the red-edge location, as presented in Fig. 1, which might be related to dissimilarity in the leaf or canopy structure. Therefore, the VIP for continuous data is sensitive to red-edge shifts. Both satellites followed the red-edge shifts to longer wavelengths by showing relatively high

Table 4
LAI prediction (validation subset) by PLS models using the entire spectra of three data formations for the seven datasets. All r values are significant ($p<0.001$). The data formation comparison presents *t*-test p values that were obtained by coupled r values from different data formations.

		Continuous	VENμS	Sentinel-2	Data formation comparison (*t*-test p values)		
					VENμS and continuous	Sentinel-2 and continuous	VENμS and Sentinel-2
2007 potato	*r*	0.92	0.93	0.92	0.75	1	0.75
	RMSEP	0.50	0.45	0.51			
2006 potato	*r*	0.65	0.80	0.80	0.13	0.13	1
	RMSEP	0.74	0.48	0.47			
All potato	*r*	0.87	0.88	0.89	0.77	0.55	0.76
	RMSEP	0.57	0.53	0.51			
2005 wheat	*r*	0.80	0.73	0.87	0.48	0.33	0.10
	RMSEP	0.82	0.82	0.75			
2004 wheat	*r*	0.82	0.91	0.94	0.05	0.002	0.26
	RMSEP	0.79	0.48	0.48			
All wheat	*r*	0.95	0.93	0.95	0.23	1	0.23
	RMSEP	0.60	0.68	0.62			
All data	*r*	0.93	0.93	0.92	1	0.50	0.50
	RMSEP	0.64	0.59	0.67			

Author's personal copy

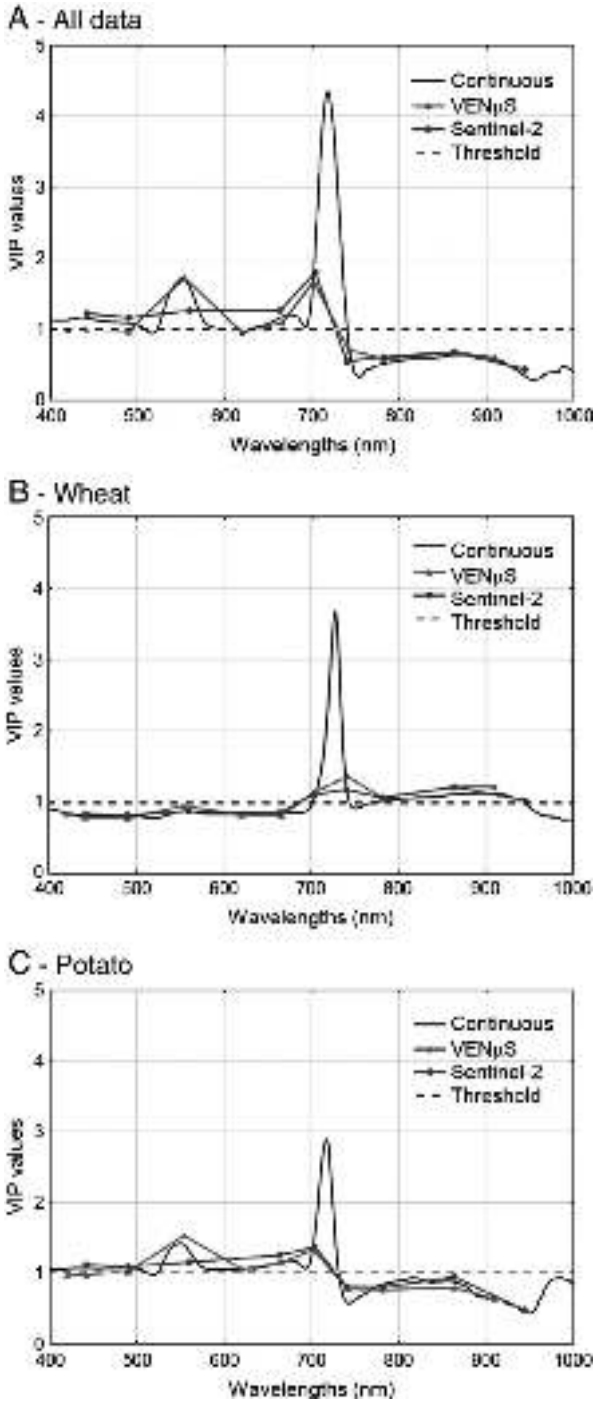

Fig. 3. VIP values as function of wavelengths formatted to continuous, VENμS, and Sentinel-2 spectra: (A) All data; (B) Wheat; and (C) Potato.

VIP values for wheat around 740 nm in Fig. 3B, bands 9 (VENμS) and 6 (Sentinel-2) and relatively high VIP values for potato around 700 nm in Fig. 3C, bands 8 (VENμS) and 5 (Sentinel-2). Therefore, based on their band settings both superspectral satellites are sensitive to shifts in the red-edge.

3.3. Vegetation indices analysis

Since the above results show that within the range of 400 to 1000 nm the red-edge is the most sensitive region to LAI for the continuous spectra and highly sensitive for the superspectral spectra, its relation to REIP and NDVI, calculated by the three data formations, should be explored. Moreover, it is also required to analyze the ability of the four red-edge VENμS bands (7 to 10 e.g., 660 to 790 nm) and Sentinel-2 bands (4 to 7 e.g., 650 to 793 nm) to predict LAI by the REIP compared to the prediction ability of the NDVI.

Fig. 4 presents the scatterplots of NDVI and REIP, computed by continuous spectra, versus LAI, for 'all data', 'all wheat', and 'all potato'. The r values are all significant ($p<0.001$). The data for the indices calculated by VENμS and Sentinel-2 provide very similar plots and r values. The 'all data' of the VENμS spectra reveal r values of 0.81, 0.70, and 0.87 for REIP, NDVI linear, and NDVI logarithmic, respectively, and of the Sentinel-2 spectra r values of 0.80, 0.70, and 0.88, respectively (scatterplots not shown). The saturation of NDVI at LAI values higher than 2, presented in Fig. 4, was expected and is in agreement with the literature. The RIEP is linearly correlated with LAI in Fig. 4A and B but in Fig. 4C slight saturation might be seen. Slight saturation of REIP when correlated with LAI was reported by Pu et al. (2003) presenting an almost linear correlation for Hyperion data of forest. Furthermore, REIP saturation at LAI values of 4 to 7, depending on chlorophyll concentration, leaf internal structure, canopy architecture and soil optical properties was reported for PROSPECT-SAIL simulations (Baret et al., 1992; Clevers et al., 2001). These results are in agreement with the appearance of the slight saturation for the 'all potato' dataset (Fig. 4C) and the linear relation for the 'all wheat' dataset (Fig. 4B) since potato and wheat are different by leaf internal structure as well as by canopy architecture. The differences in uniformity of wheat and potato are further discussed in Section 3.4. In order to address the saturation issue, it is recommended by Brantley et al. (2011) to apply indices using wavelengths in the red-edge region, since these indices are potentially more sensitive than NDVI to LAI higher than 4. Applying non-linear models for plant properties assessment and prediction can lead to uncertain predicted values (Buschmann & Nagel, 1993; Coyne et al., 2009; Ding et al., 2009; Gonzalez-Sanpedro et al., 2008; Lee et al., 2004; Li et al., 2010; Tucker, 1979; Ustin et al., 2009; Vina et al., 2004). Nevertheless, since LAI is nonlinearly related to NDVI (Clevers, 1989; Gamon et al., 1995; Haboudane et al., 2004; Myneni et al., 1997) the logarithmic relations are also presented in Fig. 4, while the results of exponential LAI prediction by NDVI are discussed later.

When each of the indices' values, calculated by continuous spectra, were related to those calculated by VENμS or Sentinel-2 spectra, the correlations are almost perfect ($r>0.99$). These results reassure the high similarity of r values for each of the indices for the three data formations and again show that there is no advantage for the continuous over the superspectral spectra. The calibration subsets of the seven datasets for both indices with respect to LAI revealed significant ($p<0.001$) r values and a high similarity between the r values of each index for the three data formations (results not shown).

Table 5 presents r and RMSEP values of LAI predicted by NDVI and REIP, computed for the validation subsets of three data formations. These results confirm the supremacy of the REIP linear prediction of LAI over the NDVI linear prediction of it, hence all r and RMSEP values of REIP are higher and lower, respectively, than those values of the NDVI. Table 5 also shows advantage of the REIP linear prediction over the NDVI exponential prediction, hence most r and RMSEP values of REIP are higher and lower, respectively, than those values of the NDVI exponential. There are 3 not significant (NS) r values in the '2005 wheat' dataset for the NDVI, probably due to the relatively small sample number for this dataset. The NDVI values, in each of the 21 cases of the exponential fitting line for calculating the predicted LAI values (data not shown) were higher than 1 already for the measured LAI values (interpolation) as well as for LAI values higher than measured (extrapolation). This is in agreement with Clevers (1989) and might make it impossible for NDVI to predict relatively high LAI values, since mathematically, the maximum measured NDVI cannot

Author's personal copy

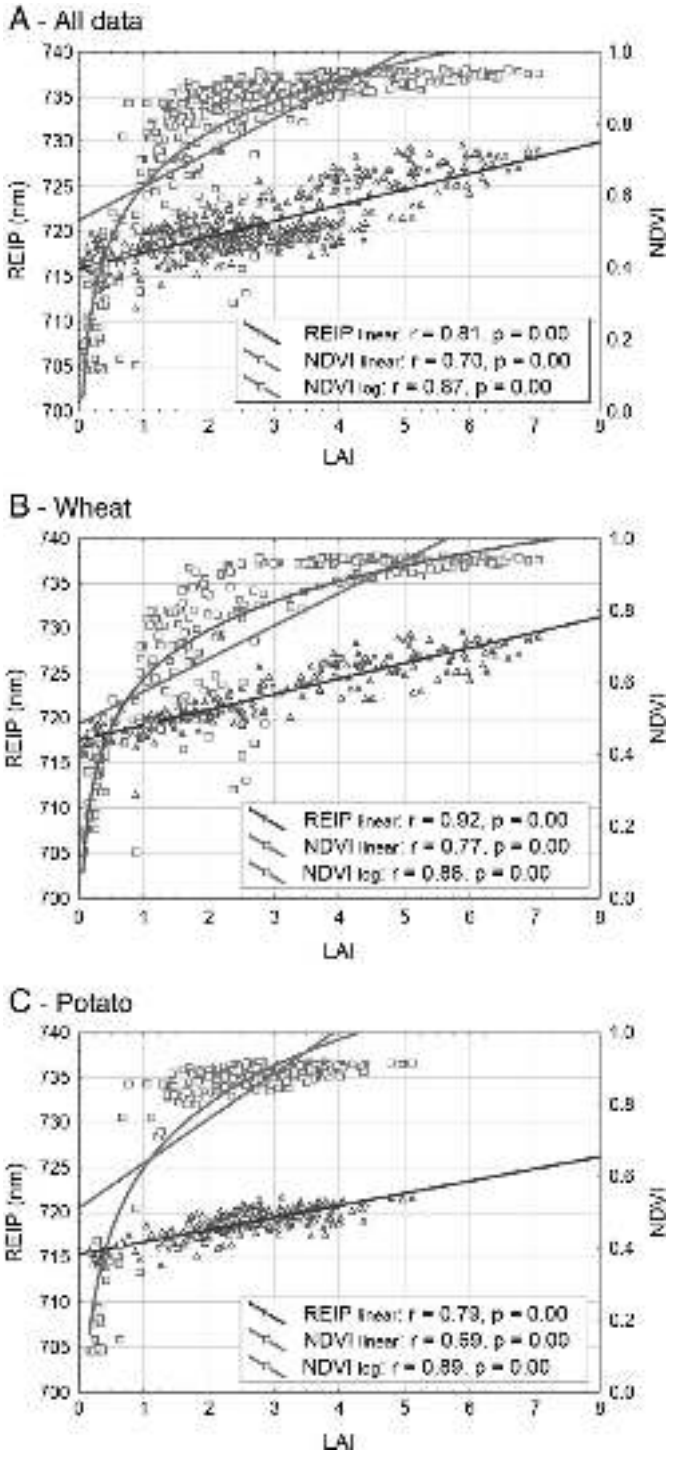

Fig. 4. LAI correlation with REIP and NDVI calculated by continuous spectra, the correlation coefficients of REIP are for linear relation and of NDVI are for linear and logarithmic relations: (A) All data; (B) Wheat; and (C) Potato.

exceed 1. In order to look for LAI prediction significant advantages, coupled r values from Table 5 were computed and presented in Tables 6 and 7. Table 6 shows that there is no significant advantage for the continuous—hyperspectral over the superspectral data formations since the *t*-test p values of the coupled data formation are all higher than 0.05. This result is prima facie not in agreement with Elvidge and Chen (1995) who presented better LAI prediction ability for NDVI computed by continuous spectra over NDVI calculated by three simulated multispectral formations: AVHRR, Landsat Multispectral

Table 5
Prediction quality of LAI by NDVI (linear and exponential) and REIP (linear) calculated by the three data formations for the seven datasets. The r values are significant ($p<0.05$) unless not significant (NS) is marked.

	Continuous			VENμS			Sentinel-2			Continuous			VENμS			Sentinel-2		
	r			*r*			*r*			RMSEP			RMSEP			RMSEP		
	NDVI Linear	NDVI Exp.	REIP Linear	NDVI Linear	NDVI Exp.	REIP Linear	NDVI Linear	NDVI Exp.	REIP Linear	NDVI Linear	NDVI Exp.	REIP Linear	NDVI Linear	NDVI Exp.	REIP Linear	NDVI Linear	NDVI Exp.	REIP Linear
2007 potato	0.70	0.77	0.85	0.70	0.77	0.84	0.71	0.77	0.85	0.76	0.71	0.57	0.76	0.70	0.59	0.76	0.70	0.58
2006 potato	0.51	0.55	0.53	0.51	0.55	0.53	0.51	0.55	0.54	0.70	0.69	0.70	0.70	0.69	0.69	0.70	0.69	0.69
All potato	0.60	0.67	0.73	0.60	0.68	0.72	0.61	0.68	0.73	0.74	0.71	0.63	0.74	0.71	0.64	0.74	0.71	0.62
2005 wheat	0.16 NS	0.17 NS	0.76	0.24 NS	0.24 NS	0.76	0.30 NS	0.29 NS	0.76	1.28 NS	1.27 NS	0.82	1.25 NS	1.43 NS	0.83	1.23 NS	1.20 NS	0.82
2004 wheat	0.70	0.80	0.81	0.70	0.80	0.82	0.71	0.81	0.81	0.91	0.77	0.84	0.90	0.76	0.79	0.89	0.74	0.82
All wheat	0.77	0.86	0.91	0.78	0.86	0.91	0.78	0.86	0.91	1.19	0.95	0.80	1.18	0.94	0.79	1.18	0.93	0.81
All data	0.70	0.78	0.77	0.70	0.78	0.78	0.71	0.79	0.75	1.03	0.89	0.91	1.03	0.89	0.91	1.02	0.87	0.95

Author's personal copy

Table 6
The *t*-test p values of coupled r values (Table 5) of the same index in different data formations. Not significant (NS) means that both r values coupled are not significant as shown in Table 5.

	Data formation comparison (*t*-test p values)								
	VENμS and continuous			Sentinel-2 and continuous			VENμS and Sentinel-2		
	NDVI Linear	NDVI Exp.	REIP Linear	NDVI Linear	NDVI Exp.	REIP Linear	NDVI Linear	NDVI Exp.	REIP Linear
2007 potato	1	1	0.87	0.93	1	1	0.93	1	0.87
2006 potato	1	1	1	1	1	0.95	1	1	0.95
All potato	1	0.90	0.89	0.92	0.90	1	0.92	1	0.89
2005 wheat	0.73 NS	0.76 NS	1	0.54 NS	0.60 NS	1	0.79 NS	0.82 NS	1
2004 wheat	1	1	0.87	0.92	0.88	1	0.92	0.88	0.87
All wheat	0.86	1	1	0.86	1	1	1	1	1
All data	1	1	0.81	0.85	0.80	0.64	0.85	0.80	0.48

Scanner (MSS), and Landsat Thematic Mapper (TM). Since Elvidge and Chen (1995) did not specified weather the difference between coupled r values for LAI prediction abilities were significant, and their prediction in general was applied for LAI values smaller than 0.5, there is no contradiction and the different conclusions are acceptable. Lee et al. (2004), in agreement with the current study, reported similar correlation between LAI (obtained by several methods) and NDVI computed by AVIRIS continuous spectra and NDVI computed by simulated Landsat enhanced Thematic Mapper Plus (ETM+) in four different plant communities, including agricultural landscape. In the current research it is shown that continuous and superspectral band formations and indices of the red-edge region can equally predict LAI, in contradiction to the findings of Lee et al. (2004), assuming that the red-edge region can only be applied for LAI assessment by hyperspectral band formation. Stagakis et al. (2010) reported that NDVI predicted LAI better than REIP, but the significance of this advantage was not mentioned. These results are based on prediction of LAI values, smaller than 3, by indices computed by the Compact High Resolution Imaging Spectrometer (CHRIS) satellite in mode 1 (62 narrow bands) for shrublands with spatial resolution larger than 30 m in nadir. The different range of LAI values and landscape engaged in the current research diminish the difference in the results, since agricultural fields are assumed to include less plant species and be more spatially uniform than shrublands.

Table 7 reveals that the REIP advantage over the NDVI is not significant in most cases. Note that the *t*-test p value is a combination of the number of samples and the difference between the coupled r values. For the NDVI linear relation with LAI, in the cases of '2005 wheat' and 'all wheat', the advantage of REIP is significant. In most of the cases the REIP has higher r values than the NDVI exponential but only in the case of '2005 wheat' this advantage is significant. REIP of the '2004 wheat' dataset has insignificantly higher r values and lower RMSEP values than the NDVI, the same trend is also seen for '2007 potato' and '2006 potato' (Table 7). In case of NDVI and REIP, it is shown that the indices derived from superspectral data perform similarly to those derived from hyperspectral data. Significant difference by t-testing (as in Tables 6 and 7) coupled r values (from Table 5) of NDVI linear and NDVI exponential was found only for the 'all wheat' and 'all data' datasets for all data formations (not presented). Therefore, for these 6 cases (3 for each dataset) the NDVI exponential advantage over the NDVI linear for LAI prediction is significant. For the rest of the 15 cases (3 for each dataset) there is no significant advantage for the NDVI exponential although it shows higher r values than the NDVI linear for all cases (Table 5).

Since the G region sensitivity to LAI changes (Fig. 3A and C) is assumed to be related to potato (hardly visible in Fig. 3B) and as presented above the LAI prediction ability is better for wheat than for potato, several VENμS-based vegetation indices correlations with LAI for 'all potato' were examined. The indices examined were: Green Normalized Difference Vegetation Index (GNDVI; Gitelson et al., 1996); Modified Chlorophyll Absorption in Reflectance Index (MCARI; Daughtry et al., 2000); Transformed Chlorophyll Absorption in Reflectance Index (TCARI; Haboudane et al., 2002); Renormalized Difference Vegetation Index (RDVI; Roujean & Breon, 1995); Modified Soil Adjusted Vegetation Index (MSAVI2; Broge & Leblanc, 2000); Total Chlorophyll Index (TCI; Coyne et al., 2009; Gitelson et al., 2003); and several ratio, difference and normalized difference vegetation indices combining mainly G and red-edge bands examined by Zarco-Tejada et al. (2005), Stagakis et al. (2010) as well as new band combinations. Although few G band indices were significantly better correlated with LAI than NDVI (data not shown) none were significantly better correlated with LAI than REIP (data not shown). Among the examined indices the TCI, a chlorophyll red-edge index, was best correlated with LAI.

3.4. Crop uniformity

Calibration of indices for a certain canopy could be unsuitable for another kind of canopy (le Maire et al., 2008), therefore it is acceptable to obtain different quality of LAI predictions from the two crops. The range of LAI values of wheat and potato are 6.99 and 4.95 and the average values are 2.92 and 2.55, respectively (Fig. 4B and C). The better LAI prediction ability of NDVI for wheat in comparison with potato (Tables 4 and 5) is in agreement with

Table 7
The *t*-test p values of coupled r values (Table 5) of the two indices (i.e., NDVI and REIP) for the same data formation.

	Indices comparison (*t*-test p values) NDVI linear and REIP linear			Indices comparison (*t*-test p values) NDVI exponential and REIP linear		
	Continuous	VENμS	Sentinel-2	Continuous	VENμS	Sentinel-2
2007 potato	0.07	0.1	0.09	0.28	0.34	0.28
2006 potato	0.90	0.90	0.84	0.90	0.90	0.94
All potato	0.14	0.15	0.14	0.43	0.60	0.50
2005 wheat	0.0008	0.002	0.005	0.0009	0.002	0.005
2004 wheat	0.17	0.12	0.20	0.88	0.76	1
All wheat	0.0005	0.001	0.001	0.11	0.11	0.11
All data	0.14	0.08	0.4	0.81	1	0.34

Author's personal copy

Aparicio et al. (2002) resulting in better LAI prediction by NDVI for a wider range of LAI values. The range of dry weight (above ground biomass dried in an oven) values for the same locations as LAI values, for wheat and potato are 934 and 279 g^{-2}, and the average values are 302 and 127 g^{-2}, respectively, determining that there is more wheat than potato per unit area in the current study. Furthermore, the correlation between dry weight and LAI for 'all potato', 'all wheat', and 'all data' datasets resulted in R^2 values of 0.61, 0.65, and 0.54, respectively, leading to the understanding that the two crops should be analyzed, and when the time comes, monitored separately.

The LAI prediction by the entire spectra as well as by the indices shows differences worth discussing. The *t*-test for coupled r values of the 'all wheat' and 'all potato' datasets from Table 5 was computed. The *t*-test p values computed for the REIP for the three data formations were lower than 0.0001 and for the linear as well as exponential NDVI continuous, VENμS, and Sentinel-2 were 0.001, 0.002, and 0.002, respectively. Since the *t*-test p values in all 9 cases are lower than 0.05, the r values are significantly different and percentage of RMSEP values (calculated as presented in Section 3.2) show advantage for the 'all wheat'. Therefore, LAI is significantly better predicted by the 'all wheat' dataset than by the 'all potato' dataset.

A general remark is that wheat and potato are different crops but a more detailed explanation is also suggested. As mentioned before, the IFOV of the reflectance measurements is ~0.35 m^2 corresponding to a diameter of 0.66 m. Since the length of the ceptometer's probe is ~130% longer than the IFOV diameter there is an advantage for LAI assessment for the more uniform crop, in this case the wheat. Uniform crop refers to the number of rows of plants growing in the IFOV: three to four rows for wheat and only less than one row for potato (the in-between row distance for wheat is around 20 cm, and around 94 cm for potato). Considering the within row spacing, the amount of plants in the IFOV is around 70 for wheat and only up to 4, most likely 1 or 2, for potato, therefore, wheat canopy covers soil more uniformly. Moreover, the LAI measurements included a non overlapping area that is not in the IFOV of the ASD. Since potato is less uniform than wheat the non overlapping area in the wheat field will be more alike the IFOV than in potato. In the potato case, in the early growing stages, it is logical to assume that the non overlapping area will mostly include soil. Therefore, potato spectra will be relatively more influenced than wheat spectra, by the soil component as shown in Fig. 2. The soil component can be seen as the reflectance curve goes upwards from G to R spectral regions, overcoming the chlorophyll absorption in the R region. The analysis of the LAI observed versus LAI predicted graphs (data not shown) by comparing slopes of trend lines, resulted in the understandings that for both crops, LAI values were underestimated, and that the wheat is less underestimated than the potato. The soil component effect in the non overlapping area mentioned above can explain some of the differences in the results between wheat and potato. Also mentioned is the wheat average above ground dry biomass per unit area that is roughly two times the potato dry biomass. Although REIP is influenced by leaf chlorophyll content (Clevers et al., 2001) and reflectance in red-edge wavelengths is sensitive to leaf chlorophyll content (Curran et al., 1992; Ding et al., 2009), Curran et al. (1990) reported that most of the red-edge variability was related to the amount of canopy within the IFOV and not to the chlorophyll content. Therefore, the REIP lesser LAI prediction ability for the potato data may be partly related to the effect of relatively lesser amount of biomass in the IFOV (i.e., potato canopy in comparison with wheat canopy). It might be that the relatively high LAI prediction ability by REIP for wheat is due to REIP correlation with LAI and chlorophyll content together. This is not the case for the potato since it has a lower amount of canopy in the IFOV that decreases the influence of chlorophyll on the REIP and therefore might be partly responsible for the reduced prediction ability.

Another issue that should be considered is the sensitivity of the field spectrometer across the IFOV (Mac Arthur et al., 2006, 2007; Milton et al., 2009). For example in early growing stages the spectra of a less uniform crop can include more or less soil than its actual relative part in the IFOV. In any case the measurements in early growing stages were included in order to provide wider variability of spectral data and to facilitate the most basic step towards satellite application by not working only with "clean" data. By similar logic to what was mentioned above, it is more probable to obtain spectral measurements that are more realistically related to the IFOV, for the more uniform crop. Again, the higher probability to get more realistic spectral measurements is for wheat. This might also explain part of the advantage in the quality of LAI prediction by spectral indices as well as by PLS model for 'all wheat' over 'all potato' datasets. Furthermore, dynamic range of an index is computed as the difference between the maximum and the minimum values of it, the wider the dynamic range, for the same bands, the more robust the index is (Gitelson, 2004). The dynamic ranges of REIP for wheat and potato are 18.1 and 6.1 nm, respectively. This goes in agreement with the finding that LAI is better predicted by REIP for wheat than for potato. The dynamic range values were obtained for all samples of continuous spectra (the values for the VENμS and Sentinel-2 are similar and therefore not presented). In general, upscaling increases errors (le Maire et al., 2008) but for the potato case it might result in better LAI prediction since it will be visible as a more uniform crop than on ground level.

3.5. Upscaling potential

In order to consider the LAI prediction by REIP potential upscaling to the future satellites VENμS and Sentinel-2, the assumed influence of properties such as: atmospheric influence (clouds), pixel size, revisit time, and viewing angle should be discussed. In order to apply automated atmospheric correction, cloud detection as a preliminary step is needed. The multi-temporal cloud detection (MTCD) to be applied for VENμS images (which might be applied for Sentinel-2) method has a low amount of false detections and is tuned to identify even thin clouds (Hagolle et al., 2010). Therefore, both satellites produce images that are assumed to provide data with minimal atmospheric influences. There is an increase in accuracy of LAI predicted by NDVI, as the pixel size increases from 2 to 4 to 8 m (Walthall et al., 2007). On the other hand Colombo et al. (2003) found no change in accuracy for pixel sizes of 12, 24, and 36 m. Since the spatial resolution of VENμS is 10 m and Sentinel-2 is 10–20 m, in the relevant bands, both sensors are in the range of the optimal LAI accuracy for NDVI. REIP is not sensitive to soil background (Baret et al., 1992; Clevers et al., 2001). Therefore both sensors are considered to provide reliable data for LAI assessment, by REIP, especially for field crops that are assumed to be a uniform target at such spatial resolutions. Stagakis et al. (2010) conducted prediction of LAI values for shrublands at different viewing angles: +55°, +36°, 0°, and −36°. It was reported that the REIP prediction in most viewing angles (+36°, 0°, and −36°) is less influenced than the +55°. The viewing angles of VENμS and Sentinel-2 are within the range of +36° to −36° with a wide range of directions. Since the viewing angle for each site will be constant there is a need to further study the viewing angle effect on vegetation indices behavior and relationships with vegetation properties, under changing temporal resolutions.

LAI retrieval for Landsat images by PROSPECT-SAIL models for several field crops was conducted and compared to LAI retrieval by NDVI and it was concluded that the main advantage of the model in comparison with the NDVI–LAI relationship is the model's ability to obtain LAI values in higher ranges that can be reached by field crops (Gonzalez-Sanpedro et al., 2008). Prediction of LAI computed from PROSAIL model by normalized difference index for Hyperion images of forest resulted in saturation for LAI values higher than 3 (le Maire et al., 2008). The red-edge region was reported by Lee et al. (2004) as more important than the NIR for LAI prediction and as presented in

Author's personal copy

the current study the REIP–LAI relationship does not show saturation. Moreover, high spatial resolution and the ability to obtain images with same viewing angle every two days are mentioned as important properties for LAI assessment from space (Gonzalez-Sanpedro et al., 2008). VENμS and Sentinel-2 will apply four red-edge bands in relatively high spatial resolution, short revisit time with constant viewing angle per site, and are therefore recommended for LAI assessment by the REIP.

4. Summary and conclusions

In order to demonstrate the ability of superspectral resolutions to assess LAI values in field crops, three spectral data formations (continuous, VENμS, and Sentinel-2) were studied, for wheat and potato crops. The relation of the data formations to LAI and its prediction by entire spectra, as well as by vegetation indices (REIP and NDVI), were explored by several methods. The VIP over the PLS analysis confirmed that the red-edge is a highly sensitive region to LAI variability in the range of 400–1000 nm. The results show that superspectral sensors can perform as well as the hyperspectral sensor in LAI prediction of field crops, wheat (grass) and potato (broad leaf). Therefore, the forthcoming superspectral sensors, VENμS and Sentinel-2, will take advantage of these results for agricultural (and related) applications. When considering the designed spatial resolutions, VENμS might potentially provide better practical application for precision agriculture. For wheat, and, to a lesser extent, for potato, it is demonstrated that the REIP is more sensitive to LAI variability than the NDVI and therefore can be implemented by the superspectral sensors for this application.

The main conclusions can be summarized as:

- LAI prediction by continuous data does not provide any significant advantage over the VENμS and Sentinel-2 resampled data. Therefore, VENμS and Sentinel-2 are as good as continuous sensors for LAI prediction by the entire spectra as well as by NDVI and REIP.
- In the range of 400–1000 nm, the red-edge is the most or second most sensitive spectral region for assessing LAI, for continuous as well as superspectral spectra. However, the degree of importance is determined by the specific band formation of the superspectral sensor as well as the crop.
- REIP is a better LAI variability predictor than NDVI since the sensitivity of the latter drops when LAI values exceed 2. Consequently, REIP can be used for predicting LAI at all growth stages together, even when high biomass and high fractional ground cover occurs.
- The REIP is a better LAI predictor for wheat than for potato. Therefore, prima facie, based on spectral assessment, this LAI monitoring potential application is more suitable for wheat than for potato.

Future directions could be to investigate the response of vegetation indices and their correlation with vegetation properties (e.g., LAI, water and nitrogen contents) under a range of constant viewing angles and short revisit times, as will be available by VENμS and Sentinel-2. The REIP computed by superspectral sensors could be also explored for other crops and natural habitats in order to provide better LAI assessments leading to productivity estimation and potentially provide an additional environmental application for the superspectral sensors beside the potential agricultural application presented here.

Acknowledgements

This research was supported in part by Research Grant Award CA-9102-06 from BARD-AAFC, The United States–Israel Binational Agricultural Research and Development Fund and Agriculture and Agri-Food, Canada; the Chief Scientist of the Israeli Ministry of Agriculture, and the Israeli Ministry of Science, Culture, and Sport. The authors would like to thank Alexander Goldberg for his indefatigable work in the field and in the lab and to express their appreciation for the vital contributions of Gadi Hadar and Ran Ferdman, the potato growers from Kibbutz Ruhama.

References

Aparicio, N., Villegas, D., Araus, J. L., Casadesus, J., & Royo, C. (2002). Relationship between growth traits and spectral vegetation indices in durum wheat. *Crop Science*, *42*, 1547–1555.

Asrar, G., Fuchs, M., Kanemasu, E. T., & Hatfield, J. L. (1984). Estimating absorbed photosynthetic radiation and leaf-area index from spectral reflectance in wheat. *Agronomy Journal*, *76*, 300–306.

Atzberger, C., Guerif, M., Baret, F., & Werner, W. (2010). Comparative analysis of three chemometric techniques for the spectroradiometric assessment of canopy chlorophyll content in winter wheat. *Computers and Electronics in Agriculture*, *73*, 165–173.

Baret, F., Jacquemoud, S., Guyot, G., & Leprieur, C. (1992). Modeled analysis of the biophysical nature of spectral shifts and comparison with information-content of broad bands. *Remote Sensing of Environment*, *41*, 133–142.

Blackburn, G. A., & Steele, C. M. (1999). Towards the remote sensing of matorral vegetation physiology: Relationships between spectral reflectance, pigment, and biophysical characteristics of semiarid bushland canopies. *Remote Sensing of Environment*, *70*, 278–292.

Bonham-Carter, G. F. (1988). Numerical procedures and computer-program for fitting an inverted Gaussian model to vegetation refelctance data. *Computers & Geosciences*, *14*, 339–356.

Brantley, S. T., Zinnert, J. C., & Young, D. R. (2011). Application of hyperspectral vegetation indices to detect variations in high leaf area index temperate shrub thicket canopies. *Remote Sensing of Environment*, *115*, 514–523.

Broge, N. H., & Leblanc, E. (2000). Comparing prediction power and stability of broadband and hyperspectral vegetation indices for estimation of green leaf area index and canopy chlorophyll density. *Remote Sensing of Environment*, *76*, 156–172.

Buschmann, C., & Nagel, E. (1993). In vivo spectroscopy and internal optics of leaves as basis for remote sensing of vegetation. *International Journal of Remote Sensing*, *14*, 711–722.

Cho, M. A., & Skidmore, A. K. (2006). A new technique for extracting the red edge position from hyperspectral data: The linear extrapolation method. *Remote Sensing of Environment*, *101*, 181–193.

Chong, I. G., & Jun, C. H. (2005). Performance of some variable selection methods when multicollinearity is present. *Chemometrics and Intelligent Laboratory Systems*, *78*, 103–112.

Clark, R. N., King, T. V. V., Ager, C., & Swayze, G. A. (1995). Initial vegetation species and senescence/stress indicator mapping in the San Luis Valley, Colorado using imaging spectrometer data. *Summitville Forum '95*, *38*, 64–69.

Clevers, J. (1989). The application of a weighted infrared-red vegetation index for estimating leaf area index by correcting for soil moisture. *Remote Sensing of Environment*, *29*, 25–37.

Clevers, J. G. P. W., de Jong, S. M., Ephama, G. F., Van der Meer, F., Bakker, W. H., Skidmore, A., et al. (2001). MERIS and the red-edge position. *International Journal of Applied Earth Observation and Geoinformation*, *3*, 313–320.

Cohen, Y., Alchanatis, V., Zusman, Y., Dar, Z., Bonfil, D. J., Karnieli, A., et al. (2010). Leaf nitrogen estimation in potato based on spectral data and on simulated bands of the VENuS satellite. *Precision Agriculture*, *11*, 520–537.

Colombo, R., Bellingeri, D., Fasolini, D., & Marino, C. M. (2003). Retrieval of leaf area index in different vegetation types using high resolution satellite data. *Remote Sensing of Environment*, *86*, 120–131.

Coyne, P. I., Aiken, R. M., Maas, S. J., & Lamm, F. R. (2009). Evaluating yieldtracker forecasts for maize in western Kansas. *Agronomy Journal*, *101*, 671–680.

Curran, P. J., Dungan, J. L., & Gholz, H. L. (1990). Exploring the relationship between reflectance red edge and chlorophyll content in slash pine. *Tree Physiology*, *7*, 33–48.

Curran, P. J., Dungan, J. L., Macler, B. A., Plummer, S. E., & Peterson, D. L. (1992). Reflectance spectroscopy of fresh whole leaves for the estimation of chemical concentration. *Remote Sensing of Environment*, *39*, 153–166.

Darvishzadeh, R., Skidmore, A., Schlerf, M., Atzberger, C., Corsi, F., & Cho, M. (2008). LAI and chlorophyll estimation for a heterogeneous grassland using hyperspectral measurements. *Isprs Journal of Photogrammetry and Remote Sensing*, *63*, 409–426.

Daughtry, C. S. T., Walthall, C. L., Kim, M. S., de Colstoun, E. B., & McMurtrey, J. E. (2000). Estimating corn leaf chlorophyll concentration from leaf and canopy reflectance. *Remote Sensing of Environment*, *74*, 229–239.

Dawson, T. P., & Curran, P. J. (1998). A new technique for interpolating the reflectance red edge position. *International Journal of Remote Sensing*, *19*, 2133–2139.

Decagon Devices, I. (2003). AccuPAR PAR/LAI ceptometer, model LP-80. *Operator's manual* (pp. 1–45). WA, USA: Pullman.

Delegido, J., Fernandez, G., Gandia, S., & Moreno, J. (2008). Retrieval of chlorophyll content and LAI of crops using hyperspectral techniques: application to PROBA/CHRIS data. *International Journal of Remote Sensing*, *29*, 7107–7127.

Ding, P., Fuchigami, L. H., & Scagel, C. F. (2009). Simple linear regression and reflectance sensitivity analysis used to determine the optimum wavelengths for the nondestructive assessment of chlorophyll in fresh leaves using spectral reflectance. *Journal of the American Society for Horticultural Science*, *134*, 48–57.

Author's personal copy

Efron, B., & Gong, G. (1983). A leisurely look at the bootstrap, the jackknife, and cross-validation. *American Statistician*, *37*, 36–48.
Elvidge, C. D., & Chen, Z. (1995). Comparison of broad-band and narrow-band red and near-infrared vegetation indices. *Remote Sensing of Environment*, *54*, 38–48.
Gamon, J. A., Field, C. B., Goulden, M. L., Griffin, K. L., Hartley, A. E., Joel, G., et al. (1995). Relationships between NDVI, canopy structure, and photosynthesis in 3 Californian vegetation types. *Ecological Applications*, *5*, 28–41.
Gausman, H. (1985). *Plant leaf optical properties in visible and near infrared light* (pp. 20–24). Lubbock: Texas Tech Press.
Gitelson, A. A. (2004). Wide dynamic range vegetation index for remote quantification of biophysical characteristics of vegetation. *Journal of Plant Physiology*, *161*, 165–173.
Gitelson, A. A., Gritz, Y., & Merzlyak, M. N. (2003). Relationships between leaf chlorophyll content and spectral reflectance and algorithms for non-destructive chlorophyll assessment in higher plant leaves. *Journal of Plant Physiology*, *160*, 271–282.
Gitelson, A. A., Kaufman, Y. J., & Merzlyak, M. N. (1996). Use of a green channel in remote sensing of global vegetation from EOS-MODIS. *Remote Sensing of Environment*, *58*, 289–298.
Gonzalez-Sanpedro, M. C., Le Toan, T., Moreno, J., Kergoat, L., & Rubio, E. (2008). Seasonal variations of leaf area index of agricultural fields retrieved from Landsat data. *Remote Sensing of Environment*, *112*, 810–824.
Guyot, G., & Baret, F. (1988). Utilisation de la haute resolution spectrale pour suivre l'etat des couverts vegetaux. *4th International Colloquium "Spectral signatures of objects in remote sensing"* (pp. 279–286).
Haboudane, D., Miller, J. R., Pattey, E., Zarco-Tejada, P. J., & Strachan, I. B. (2004). Hyperspectral vegetation indices and novel algorithms for predicting green LAI of crop canopies: Modeling and validation in the context of precision agriculture. *Remote Sensing of Environment*, *90*, 337–352.
Haboudane, D., Miller, J. R., Tremblay, N., Zarco-Tejada, P. J., & Dextraze, L. (2002). Integrated narrow-band vegetation indices for prediction of crop chlorophyll content for application to precision agriculture. *Remote Sensing of Environment*, *81*, 416–426.
Hagolle, O., Huc, M., Pascual, D. V., & Dedieu, G. (2010). A multi-temporal method for cloud detection, applied to FORMOSAT-2, VEN mu S, LANDSAT and SENTINEL-2 images. *Remote Sensing of Environment*, *114*, 1747–1755.
Hansen, P. M., & Schjoerring, J. K. (2003). Reflectance measurement of canopy biomass and nitrogen status in wheat crops using normalized difference vegetation indices and partial least squares regression. *Remote Sensing of Environment*, *86*, 542–553.
Hatchell, D. C. (1999). *Analytical Spectral Devices, Inc. (ASD) Technical Guide.*
Herrmann, I., Karnieli, A., Bonfil, D. J., Cohen, Y., & Alchanatis, V. (2010). SWIR-based spectral indices for assessing nitrogen content in potato fields. *International Journal of Remote Sensing*, *31*, 5127–5143.
Jorgensen, R. N. (2002). Study on line imaging spectroscopy as a tool for nitrogen diagnostics in precision farming, PhD Thesis. *Agricultural Sciences Plant Nutrition and Soil Fertility Laboratory PhD*, 94.
Kimura, R., Okada, S., Miura, H., & Kamichika, M. (2004). Relationships among the leaf area index, moisture availability, and spectral reflectance in an upland rice field. *Agricultural Water Management*, *69*, 83–100.
le Maire, G., Francois, C., Soudani, K., Berveiller, D., Pontailler, J. Y., Breda, N., et al. (2008). Calibration and validation of hyperspectral indices for the estimation of broadleaved forest leaf chlorophyll content, leaf mass per area, leaf area index and leaf canopy biomass. *Remote Sensing of Environment*, *112*, 3846–3864.
Lee, K. S., Cohen, W. B., Kennedy, R. E., Maiersperger, T. K., & Gower, S. T. (2004). Hyperspectral versus multispectral data for estimating leaf area index in four different biomes. *Remote Sensing of Environment*, *91*, 508–520.
Li, F., Miao, Y. X., Hennig, S. D., Gnyp, M. L., Chen, X. P., Jia, L. L., et al. (2010). Evaluating hyperspectral vegetation indices for estimating nitrogen concentration of winter wheat at different growth stages. *Precision Agriculture*, *11*, 335–357.
Mac Arthur, A. A., Maclellan, C., & Malthus, T. J. (2006). What does the spectrometer see? *The annual conference of the remote sensing and photogrammetry society*.
Mac Arthur, A. A., Maclellan, C., & Malthus, T. J. (2007). Determining the FOV and directional response of field spectroradiometers. *The 5th EARSeL Workshop on Imaging Spectroscopy*.
McCoy, R. M. (2005). *Field methods in remote sensing* (pp. 71–88). New York: The Guilford Press.
Milton, E. J., Schaepman, M. E., Anderson, K., Kneubuhler, M., & Fox, N. (2009). Progress in field spectroscopy. *Remote Sensing of Environment*, *113*, S92–S109.
Mohd-Shafri, H. Z., Mohd-Salleh, M. A., & Ghiyamat, A. (2006). Hyperspectral remote sensing of vegetation using red edge position techniques. *American Journal of Applied Sciences*, *3*, 1864–1871.
Moran, M. S., Maas, S. J., Vanderbilt, V. C., Barnes, M., Miller, S. N., & Clarke, T. R. (2004). Application of image-based remote sensing to irrigated agriculture. In S. L. Ustin (Ed.), *Remote sensing for natural resource management and environmental monitoring, Manual of remote sensing* (pp. 617–676). Hoboken: John Wiley & sons.
Mutanga, O., & Skidmore, A. K. (2007). Red edge shift and biochemical content in grass canopies. *Isprs Journal of Photogrammetry and Remote Sensing*, *62*, 34–42.
Myneni, R. B., Nemani, R. R., & Running, S. W. (1997). Estimation of global leaf area index and absorbed par using radiative transfer models. *IEEE Transactions on Geoscience and Remote Sensing*, *35*, 1380–1393.
Nguyen, H. T., & Lee, B. W. (2006). Assessment of rice leaf growth and nitrogen status by hyperspectral canopy reflectance and partial least square regression. *European Journal of Agronomy*, *24*, 349–356.
Pimstein, A., Bonfil, D. J., Mufradi, I., & Karnieli, A. (2007a). Spectral index for assessing heading timing of spring wheat grown under semi-arid conditions. *6th European Conference on Precision Agriculture* (pp. 663–669).
Pimstein, A., Eitel, J. U. H., Long, D. S., Mufradi, I., Karnieli, A., & Bonfil, D. J. (2009). A spectral index to monitor the head-emergence of wheat in semi-arid conditions. *Field Crops Research*, *111*, 218–225.
Pimstein, A., Karnieli, A., & Bonfil, D. J. (2007b). Wheat and maize monitoring based on ground spectral measurements and multivariate data analysis. *Journal of Applied Remote Sensing*, *1* Article number 013530.
Pu, R. L., Gong, P., Biging, G. S., & Larrieu, M. R. (2003). Extraction of red edge optical parameters from Hyperion data for estimation of forest leaf area index. *IEEE Transactions on Geoscience and Remote Sensing*, *41*, 916–921.
Raven, P. H., Everet, R. F., & Eichhorn, S. E. (2005). *Biology of plants* (pp. 35–88). New-York: W. H. Freeman and Company.
Roujean, J. L., & Breon, F. M. (1995). Estimating PAR absorbed by vegetation from bidirectional reflectance measurements. *Remote Sensing of Environment*, *51*, 375–384.
Rouse, J. W., Haas, R. H., Schell, J. A., & Deering, D. W. (1974). Monitoring vegetation systems in the Great Plains with ERTS. *Third Earth Resources Technology Satellite-1* (pp. 309–317).
Stagakis, S., Markos, N., Sykioti, O., & Kyparissis, A. (2010). Monitoring canopy biophysical and biochemical parameters in ecosystem scale using satellite hyperspectral imagery: An application on a *Phlomis fruticosa* Mediterranean ecosystem using multiangular CHRIS/PROBA observations. *Remote Sensing of Environment*, *114*, 977–994.
Tarpley, L., Reddy, K. R., & Sassenrath-Cole, G. F. (2000). Reflectance indices with precision and accuracy in predicting cotton leaf nitrogen concentration. *Crop Science*, *40*, 1814–1819.
Tucker, C. J. (1979). Red and photographic infrared linear combinations for monitoring vegetation. *Remote Sensing of Environment*, *8*, 127–150.
Ustin, S. L., Gitelson, A. A., Jacquemoud, S., Schaepman, M., Asner, G. P., Gamon, J. A., et al. (2009). Retrieval of foliar information about plant pigment systems from high resolution spectroscopy. *Remote Sensing of Environment*, *113*, S67–S77.
Verhoef, W. (1984). Light-scattering by leaf layers with application to canopy reflectance modeling—The SAIL model. *Remote Sensing of Environment*, *16*, 125–141.
Vina, A., Gitelson, A. A., Rundquist, D. C., Keydan, G., Leavitt, B., & Schepers, J. (2004). Remote sensing—Monitoring maize (*Zea mays* L.) phenology with remote sensing. *Agronomy Journal*, *96*, 1139–1147.
Walthall, C. L., Pachepsky, Y., Dulaney, W. P., Timlin, D. J., & Daughtry, C. S. T. (2007). Exploitation of spatial information in high resolution digital imagery to map leaf area index. *Precision Agriculture*, *8*, 311–321.
Watson, D. J. (1947). Comparative physiological studies in the growth of field crops I. Variation in net assimilation rate and leaf area between species and varieties, and within and between years. *Annals of Botany*, *11*, 41–76.
Wold, S., Johansson, E., & Cocchi, M. (1993). PLS—Partial least squares projections to latent structures. In H. Kubinyi (Ed.), *3D QSAR in drug design: theory, methods, and applications* (pp. 523–550). Leiden: ESCOM.
Wold, S., Sjostrom, M., & Eriksson, L. (2001). PLS-regression: A basic tool of chemometrics. *Chemometrics and Intelligent Laboratory Systems*, *58*, 109–130.
Ye, X. J., Sakai, K., Okamoto, H., & Garciano, L. O. (2008). A ground-based hyperspectral imaging system for characterizing vegetation spectral features. *Computers and Electronics in Agriculture*, *63*, 13–21.
Zarco-Tejada, P. J., Ustin, S. L., & Whiting, M. L. (2005). Temporal and spatial relationships between within-field yield variability in cotton and high-spatial hyperspectral remote sensing imagery. *Agronomy Journal*, *97*, 641–653.